

Manuscript Number: MARSYS-D-11-00280

Title: On the compressibility of the surface currents in the Gulf of Finland, the Baltic Sea

Article Type: Special Issue:BSSC-2011

Keywords: compressibility; Lagrangian transport; pollution dispersion; patchiness; pollution control; Baltic Sea; Gulf of Finland

Corresponding Author: Mr. Andrea Giudici, M.Sc.

Corresponding Author's Institution: Tallinn University of Technology

First Author: Jaan Kalda, D.A.

Order of Authors: Jaan Kalda, D.A.; Tarmo Soomere, Prof.; Andrea Giudici, M.Sc.

**Abstract:** We study the effects of compressibility of a two-dimensional (2D) velocity field on the transport and mixing of substances floating on the sea surface overlying 3D circulation. The test area is the Gulf of Finland, the Baltic Sea, where large variations in compressibility are likely. The key development is the introduction of a modified measure of compressibility that is directly related to the ability of clustering of passive tracers in some regions of the sea surface. This measure is calculated based on 3D velocity fields calculated using the Rossby Centre Ocean Model (Swedish Meteorological and Hydrological Institute) for 1991 and the TRACMASS code for tracking Lagrangian trajectories. For the first time, a compressibility map of a marine region has been calculated in a systematic manner. The level of compressibility reaches the critical value for the formation of patches usually in coastal regions but also in certain elongated offshore areas. The spatial distributions of compressibility reveal extensive seasonal-scale variations, with the most persistent areas of high compressibility in the windy season (October-December).

1 On the compressibility of the surface currents in the Gulf of Finland,  
2 the Baltic Sea

3 Jaan Kalda<sup>a</sup>, Tarmo Soomere<sup>a,b</sup>, Andrea Giudici<sup>a,\*</sup>,

4 <sup>a</sup> Institute of Cybernetics at Tallinn University of Technology, Akadeemia tee 21, 12618  
5 Tallinn, Estonia

6 <sup>b</sup> Estonian Academy of Sciences, Kohtu 6, 10130 Tallinn, Estonia

7 \* Corresponding author, e-mail: andrea@cens.ioc.ee

8

9 **Abstract.** We study the effects of compressibility of a two-dimensional (2D) velocity field on  
10 the transport and mixing of substances floating on the sea surface overlying 3D circulation.  
11 The test area is the Gulf of Finland, the Baltic Sea, where large variations in compressibility  
12 are likely. The key development is the introduction of a modified measure of compressibility  
13 that is directly related to the ability of clustering of passive tracers in some regions of the sea  
14 surface. This measure is calculated based on 3D velocity fields calculated using the Rossby  
15 Centre Ocean Model (Swedish Meteorological and Hydrological Institute) for 1991 and the  
16 TRACMASS code for tracking Lagrangian trajectories. For the first time, a compressibility  
17 map of a marine region has been calculated in a systematic manner. The level of  
18 compressibility reaches the critical value for the formation of patches usually in coastal  
19 regions but also in certain elongated offshore areas. The spatial distributions of  
20 compressibility reveal extensive seasonal-scale variations, with the most persistent areas of  
21 high compressibility in the windy season (October–December).

22

23 *Keywords:* compressibility; Lagrangian transport; pollution dispersion; patchiness; pollution  
24 control; Baltic Sea; Gulf of Finland

25

26 *Highlights:*

- 27 ■ We develop a modified measure of compressibility of sea surface reflecting clustering  
28 of tracers
- 29 ■ Compressibility maps for the Gulf of Finland are calculated in a systematic manner
- 30 ■ We track areas of a marine region which are likely to form clusters of floaters
- 31 ■ High compressibility identified near the River Neva mouth
- 32 ■ Extensive seasonal-scale variability in compressibility in the Gulf of Finland

33

34 **1. Introduction**

35 Knowledge of fundamental features of pollution behaviors and impacts on marine  
36 environment is crucial for sustainable management of vulnerable sea areas. This knowledge is  
37 of key importance not only for a better understanding of the environmental responses to  
38 pollutants but even more for the development of efficient prevention measures. This  
39 knowledge is still sparse, and many factors are yet to be taken into account (Andrady, 2011;  
40 Schilling and Zessner, 2011). One of the vital questions is how and where dangerous

41 concentrations of adverse impacts (e.g. harmful algal blooms), frequently observed in natural  
42 conditions in the surface layer, develop from overall low readings of background fields.

43 The movement of different substances within the water column in the ocean is  
44 governed by the three-dimensional system of currents. Such motions generally result in  
45 spreading of initially closely located particles (Richardson, 1926; Ollitrault et al., 2005).  
46 Therefore, it is natural to expect that the concentration of different adverse impacts is the  
47 largest in the vicinity of their release site to the marine environment and that remote areas are  
48 safe. The situation is much more complicated for substances (such as oil pollution or plastic  
49 debris) that are locked in the surface layer. First of all, this layer is additionally affected by  
50 wind and waves. Both wind- and wave-induced transport are highly anisotropic and mostly  
51 mimic the behavior of the wind and wave patterns, which can be forecast and hindcast with a  
52 reasonable accuracy nowadays. As the properties of both these fields usually vary quite  
53 slowly over the open sea areas, the related transport normally does not lead to substantial  
54 changes in the concentration of different substances in the surface layer.

55 It is well known that large intense currents such as the Gulf Stream or Kuroshio carry  
56 large water masses from coastal areas across oceans to a distance of many 1000s of km. This  
57 feature makes the pollution or litter propagation problem a fairly general and global one.  
58 Moreover, substances in the surface layer are carried to extremely remote locations over areas  
59 that do not host such strong currents. For example, debris originating from South America is  
60 frequently found as beach litter on remote Pacific Islands (Richards, 2011).

61 A fascinating property of marine debris is its ability to form areas with high  
62 concentrations in the open ocean, far from jet currents. Perhaps the most well-know such area  
63 is located in the North Pacific Subtropical Convergence Zone (STCZ) and is sometimes called  
64 the Great Pacific Ocean Garbage Patch (Pichel, 2007). Therefore, even remote offshore  
65 locations are certainly not immune from problems related to high readings of pollution or  
66 litter in the surface layer.

67 The existence of such areas is usually associated with specific three-dimensional (3D)  
68 features of the ocean circulation (Lee, 2010). In essence, this feature can be interpreted as a  
69 particular realization of so-called patchiness of a number of different properties of the marine  
70 environment (Powell and Okubo, 1994). Many physical processes may be responsible for the  
71 presence of patches of different size and shape. For example, filament generation in quasi-  
72 two-dimensional velocity field (Held et al., 1995) naturally leads to extremely complicated  
73 spatial structure of concentrations of various properties (Kalda, 2000) and even such  
74 frequently occurring phenomena as horizontal density gradient (Burchard et al., 2008) or  
75 classical estuacione circulation (Burchard et al., 2004) may lead to accumulation of sediment  
76 particles or well-defined turbidity maxima. In the Baltic Sea patchiness has been subject to  
77 intense studies since the 1980s (Kononen et al., 1992; Granskog et al., 2005). In this area the  
78 phenomenon of patchiness is usually linked to various mesoscale hydrodynamic features such  
79 as eddies, frontal zones, or local jet currents. A similar mechanism, usually working at even  
80 smaller scales, is Langmuir circulation (Thorpe, 2009). All the listed phenomena normally  
81 have a substantial vertical component and, thus, an essentially 3D vertical structure.

82 In this paper, we make an attempt to link the potential of formation of patches (more  
83 generally, inhomogeneities in initially homogeneously distributed fields of passive tracers  
84 locked in the surface layer) on sea surface with so-called property of compressibility of sea  
85 surface. This property is one of important factors, which controls the behavior of the pollution  
86 spreading, and, if present, may naturally lead to the formation of high concentrations in  
87 different adverse impacts or marine garbage. We emphasize the substantial difference of this  
88 phenomenon from the more widely spread concept of compressibility of the entire medium

89 (sea water or air) understood as a measure of the relative volume change as a response to  
90 pressure variations. In this paper we use the notion of compressibility as the relative weight of  
91 the potential component of a velocity field. This definition relies on the motion of water  
92 particles. Three-dimensional atmospheric flows as well as the flows in the bulk of the water  
93 basins are usually almost incompressible; however, the two-dimensional velocity field at the  
94 water surface can be compressible even when water particles, initially located at the surface,  
95 are confined to stay at the surface. This happens because of the possibility of vertical motions  
96 of water masses (up- and down-welling in the marine environment) in the water column. In  
97 this sense, compressibility of sea surface can be interpreted as an indicator of the impact of  
98 3D motions on the concentrations of different substances in a particular location of the  
99 surface. The highest values of compressibility can, thus, be naturally associated with areas  
100 prone to the development of well-defined patches.

101 While the effect of compressibility on different properties of the fluid motion and  
102 transport has been extensively studied both theoretically and experimentally (Falkovich et al,  
103 2001; Cressman et al., 2004; Boffetta et al., 2004; Kalda, 2007), the evidence of its  
104 importance in marine environments is still scarce. The most prominent consequence of  
105 compressibility is the gathering of floating particles into patches. This feature is crucial in  
106 many environmental applications as it may substantially affect both the probability and  
107 propagation time of adverse impacts in different offshore areas to the vulnerable regions; for  
108 example, pollution is likely to stay for a long time in areas of high compressibility. Such areas  
109 can be interpreted as natural areas of reduced risk in terms of pollution transport from these to  
110 the coasts (Soomere et al., 2010).

111 In this paper, we study the effects of compressibility of a two-dimensional velocity  
112 field on the transport and mixing of substances floating on the sea surface of the Baltic Sea, in  
113 the area of the Gulf of Finland, and overlying a 3D field of motions. The key development is  
114 the introduction of a modified measure of compressibility (that is directly related to the ability  
115 of clustering of passive tracers in some regions of the sea surface) and a demonstration that its  
116 values may exceed the threshold for the formation of patches. The structure of the paper is as  
117 follows. Section 2 gives a short insight into the general problem of compressibility of 2D and  
118 3D flows. The pool of velocity data, models used for its calculation and for tracking the  
119 surface elements on sea surface are described in Section 3. The definition of a modified  
120 measure for compressibility of 2D flows and its calculation scheme from 2D velocity fields  
121 are presented in Section 4. Section 5 depicts the resulting spatial distribution of this measure  
122 for the Gulf of Finland. The basic message from the research to the marine science is  
123 formulated in Section 6.

124

## 125 **2. Compressibility of 2D flows overlying almost incompressible 3D motions**

126 The fundamental theorem of vector calculus, the Helmholtz's theorem, states that any  
127 sufficiently smooth, rapidly decaying vector field in three dimensions can be expressed as the  
128 sum of an irrotational (curl-free, also called potential) vector field and a solenoidal  
129 (divergence-free) vector field. This is known as the Helmholtz decomposition. Consequently,  
130 virtually every realistic field of motions in the ocean (formally, defined everywhere in space  
131 and vanishing at infinity together with its first derivatives) can be decomposed, to a first  
132 approximation, into its solenoidal and potential components (with zero divergence and curl,  
133 respectively). In this framework, compressibility is defined as the relative weight of the  
134 potential component of the velocity field. Its particular values, therefore, are in the range from  
135 0 (fully solenoidal flow) to 1 (fully potential flow). In what follows, however, we adopt a  
136 slightly different definition of compressibility, which will be referred to as the *finite-time*

137 *compressibility* and which coincides with the classical definition at the limit of ideal  
138 Kraichnan flows (Falkovich et al., 2001). The reasons for such an approach will be explained  
139 below.

140         There exists a direct link between the compressibility of a motion system (either 2D or  
141 3D) and the possibility of formation of patches of concentration of passive tracers or particles  
142 injected into the fluid. Namely, systematic development of patches is only possible if the  
143 potential flow component dominates, that is, the values of compressibility exceed the  
144 threshold of 0.5. Compressibility of a realistic fluid motion is generally nearly 0, hence fluids  
145 are incapable of producing the patchiness of tracers (Fine and Millero, 1973). The most  
146 important exception here is the marine surface layer. Here large values of compressibility are  
147 possible due to the capability of the particles floating on it to “dive” into the third dimension  
148 (Garrison, 2011). Thus, the average compressibility of such a formally 2D velocity field on  
149 sea surface may largely exceed the analogous values for purely 2D or geostrophic flow. This  
150 property, in essence, is a generalization of several above-mentioned phenomena that lead to  
151 the development of inhomogeneities on the sea surface and can explain, at least partially, the  
152 patchiness of floaters in the marine environment.

153         It has been shown that the presence of non-zero compressibility can affect  
154 dramatically the behavior of the tracers, giving rise to clusterization of the tracer particles and  
155 fractal structures (Bec et al., 2004; Perlekar et al., 2010). According to the theoretical studies  
156 of ideal Kraichnan flows (which are delta-correlated in time), the crossover to clusterization  
157 takes place at the critical value compressibility of  $C = 0.5$  (Falkovich et al., 2001). However,  
158 both experimental and numerical results indicate that the time correlations (which are always  
159 present for real hydrodynamic flows) can either inhibit or catalyze the clusterization process  
160 (Boffetta et al., 2004). Regarding the compressibility of real water flows, it has been shown  
161 that the free-slip surface of fully turbulent water volumes is characterized by  $C \approx 0.5$   
162 (Schumacher and Eckhardt, 2002). However, mesoscale and large-scale marine water flows  
163 are often quasi-two-dimensional (Rhines, 1979; Kraichnan and Montgomery, 1980), which  
164 leads to the reduction of the compressibility of the surface velocity field. Theoretically, non-  
165 linear waves may contribute to the increase in the surface compressibility. This effect  
166 apparently becomes evident, if at all, in quite specific conditions. For example, it has been  
167 shown that such an effect is negligible for weakly nonlinear waves (Vucelja et al., 2007).  
168 Therefore, the major source of sea surface compressibility evidently is the specific nature of  
169 the local 3D circulation that may give rise to systematic diving (e.g. downwelling) or uplift  
170 (e.g. upwelling) of water masses in certain sea areas.

171         The compressibility of a velocity field coincides with that of the motion of fluid  
172 particles floating in it. This feature makes it possible to analyze the compressibility of the  
173 particle field by means of addressing the compressibility of the vector field consisting of  
174 displacement vectors of simulated floaters’ trajectories.

175         Since the overall surface area of the sea is constant in time, the average flow  
176 divergence over the entire sea surface is strictly zero. Surface floaters (passive tracers, adverse  
177 impacts, plastic debris, oil pollution, etc.) though, tend to spend more time in contracting  
178 regions than in expanding ones: the expanding flows tend to push floaters away, while the  
179 contracting ones tend to attract and keep floaters within their areas of influence. Therefore,  
180 particles tend to gather into patches in areas that systematically reveal nonzero  
181 compressibility.

182

183 **3. Circulation model and Lagrangian tracking code**

184 In this study we concentrate on the Gulf of Finland (Alenius et al., 1998), the  
185 easternmost sub-basin of the Baltic Sea. This water body frequently hosts long-term powerful  
186 upwelling and downwelling events (Lehmann and Myrberg, 2008; Leppäranta and Myrberg,  
187 2009) and thus is a natural candidate for sea domains with substantial nonzero levels of  
188 surface compressibility. We employ surface velocity fields calculated for 1987–1991 in the  
189 Swedish Meteorological and Hydrological Institute by the Rossby Centre Ocean Model  
190 (RCO) in the framework of BONUS+ BalticWay cooperation (Soomere et al., 2010). This  
191 time interval has been chosen in order to make our results comparable with those obtained in  
192 the framework of studies into the quantification of offshore areas in terms of their ability to  
193 serve as sources of environmental risk to the coastal areas in terms of current-induced  
194 transport of adverse impacts released at these areas to the nearshore (Soomere et al., 2011).  
195 The horizontal resolution of the model grid is 2×2 nautical miles and the model uses 41  
196 vertical levels in  $z$ -coordinates (Meier et al., 2003; Meier, 2007). The thickness of the vertical  
197 layers varies between 3 m close to the surface and 12 m in 250 m depth. The uppermost layer  
198 corresponds to water masses at depths 0–3 m.

199 The RCO model has been described in a number of sources (Meier, 2001; Meier et al.,  
200 2003). As we only use velocity fields produced using this model, we present here only shortly  
201 its key features. It is a Bryan-Cox-Semtner primitive equation circulation model following  
202 (Webb *et al.*, 1997) with a free surface (Killworth et al., 1991) and open boundary conditions  
203 (Stevens, 1991) in the northern Kattegat. It is coupled to a Hibler-type sea ice model (Hibler,  
204 1979) with elastic-viscous-plastic rheology (Hunke and Dukowicz, 1997). Subgrid-scale  
205 mixing is parameterized using a turbulence closure scheme of the  $k$ - $\epsilon$  type with flux boundary  
206 conditions to include the effect of a turbulence-enhanced layer due to breaking surface gravity  
207 waves (Meier, 2001). A flux-corrected, monotonicity-preserving transport scheme following  
208 (Gerdes et al., 1991) is embedded. No explicit horizontal diffusion is applied. The model run,  
209 data from which is used below, is forced with 10 m wind, 2 m air temperature, 2 m specific  
210 humidity, precipitation, total cloudiness and sea level pressure fields from a regionalization of  
211 the ERA-40 re-analysis over Europe using a regional atmosphere model with a horizontal  
212 resolution of 22 km during 1961–2007 (Samuelsson et al., 2011). The atmospheric forcing  
213 fields are extended beyond the ERA-40 period with analysis data from the operational  
214 ECMWF model (Anderson et al., 2006). As the atmospheric model tends to underestimate  
215 wind speed extremes, the wind is adjusted using simulated gustiness to improve the wind  
216 statistics (Samuelsson et al. 2011). Standard bulk formulae are used to calculate the air-sea  
217 fluxes over open water and over sea ice. For further details of the model set-up and an  
218 extensive validation of model output the reader is referred (Meier, 2001; Meier et al., 2003)).

219 The displacement of water particles has been calculated using their Lagrangian  
220 trajectories found by the TRACMASS model (Blanke and Raynard, 1997; Döös, 1995; de  
221 Vries and Döös, 2001) from the precomputed RCO velocity fields. Theoretically, using the  
222 TRACMASS model together with the 3D velocity data, it would be possible to calculate the  
223 classical compressibility of the velocity fields. However, as mentioned above, for real time-  
224 correlated flows, the non-zero values of compressibility alone are unable to describe the  
225 development of patches on the sea surface (such as the floater clusterization). The physical  
226 reason for that is most explicitly demonstrated when we consider a hypersonic (compressible)  
227 gas flow. In such flows, at any moment of time, the velocity field is compressible, because the  
228 dynamic pressure exceeds the hydrostatic one. Meanwhile, this compressibility has long-term  
229 negative correlation. For delta-correlated flows, nonzero values of compressibility mean that  
230 the sum of Lyapunov exponents is negative, i.e. material volumes contract exponentially in  
231 time. This contraction is actually the fundamental reason of the creation of patchiness owing  
232 to the presence of non-zero compressibility. However, the material volumes of hypersonic gas

233 flow cannot contract exponentially: eventually the hydrodynamic pressure will play a role and  
 234 stop the contraction. As a result, even though the classical compressibility of hypersonic  
 235 flows can be considerable, the sum of the Lyapunov exponents remains strictly equal to zero.  
 236 This property is equivalent to the absence of creation of long-term patchiness.

237

#### 238 **4. Method for compressibility calculations**

239 Therefore, in order to reach a measure of compressibility that is more directly related  
 240 to the formation of patches, the definition of compressibility needs to be revised towards  
 241 accounting for the properties of real flows with finite time-correlations. Following this line of  
 242 thinking, we employ the modified definition of (finite-time) compressibility. The idea is to  
 243 relate the finite-time changes in the material volumes (e.g., surface areas in the case of 2D  
 244 flows overlying 3D circulation) to the finite-time changes in the separation between material  
 245 particles. The modification is consistent in the sense that the introduced measure coincides  
 246 with the values of the classical compressibility at the limit of infinitesimally small time  
 247 windows and Kraichnan flows.

248 The basic idea in the calculations is to look at the changes in the surface of small  
 249 elements of the surface. The simplest element is formed by three points at the surface,  
 250 forming a triangle with nonzero area (Fig. 1). The displacement of its vertices is tracked using  
 251 the trajectory simulation code TRACMASS.

252 The changes to the position of the vertices were obtained by running TRACMASS for  
 253 a cluster of passive tracers associated water particles placed in the center of each grid point.  
 254 The initial separation of the neighboring tracers along latitudes and along longitudes is,  
 255 therefore, about 2 nautical miles. Simulations are run over a data set which contains  
 256 information data for the year 1991. Tracers are repositioned in the center of their belonging  
 257 grid cell at the end of a 24 hours run. From these simulations, we retrieve a displacement  
 258 vector field of tracers' positions, which is used to calculate a compressibility value for each  
 259 grid cell. This value is calculated in terms of patches' properties.

260 Let us consider a grid cell, at time step 0 for a given day. As a simplest surface  
 261 element representing the change in the surface area at this point, we choose a triangle  
 262 consisting of this point and its immediate neighbor to the south and east (Fig. 1). This stencil  
 263 is applied to the entire surface of the Gulf of Finland and its entrance area. More formally, let  
 264  $(x_1^t, y_1^t)$ ,  $(x_2^t, y_2^t)$  and  $(x_3^t, y_3^t)$  be the coordinates of the vertices of an element at time step  $t$ . It  
 265 is convenient to consider twice the surface of an element  $S_t$ , expressed at time step  $t$  as  
 266 follows:

$$S_t = |(x_1^t - x_2^t) \cdot (x_1^t - x_3^t) \cdot (y_1^t - y_3^t) \cdot (y_1^t - y_2^t)|. \quad (1)$$

267 The relative change over time of its area is  $dS_t = (S_t - S_{t-1})/S_t$ . Another component of  
 268 our definition of compressibility is the squared length of two edges of the element:

$$A_t = (x_1^t - x_2^t)^2 + (y_1^t - y_2^t)^2; B_t = (x_1^t - x_3^t)^2 + (y_1^t - y_3^t)^2 \quad (2)$$

269 Their respective changes over time are obviously  $dA_t = (A_t - A_{t-1})/A_t$  and  
 270  $dB_t = (B_t - B_{t-1})/B_t$ . The finite-time compressibility value is calculated now from the  
 271 changes to the three quantities in question at different time steps as follows:

$$C = \frac{2dS_{rms}}{dA_{rms} + dB_{rms}}, \quad (3)$$

272 where the components of the right-hand side of Eq. (3) have the meaning of rms (root mean  
273 square) values of the respective quantities

$$dS_{rms} = \sqrt{\frac{1}{n} \sum_i^n dS_i^2}, \quad dA_{rms} = \sqrt{\frac{1}{n} \sum_i^n dA_i^2}, \quad dB_{rms} = \sqrt{\frac{1}{n} \sum_i^n dB_i^2} \quad (4)$$

274 and  $i$  indicates a particular realization of the flow. The rms in Eqs. (4) is calculated on a  
275 number of samples that linearly depends on the size of the chosen time window. This is a  
276 direct consequence of the fact that running a simulation over a longer time window, produces  
277 a higher number of samples. It is, however, obvious that the limiting values of  $C$  in Eq. (3) do  
278 not depend on the number of samples provided the velocity field is statistically stationary.

279 From Eqs. (1)–(4) it follows that if the flow is purely incompressible,  $dS_{rms} = 0$ , and  
280 hence the compressibility  $C = 0$  in the entire volume filled (or area covered) by such a flow.  
281 In the contrary, if the flow is purely contractive or expanding, the quantities  $A$  or  $B$  would  
282 change with the same relative rate as  $S$ , so that we would have  $C = 1$ . The values of  $C$  defined  
283 by Eq. (3) obviously lie in the range  $[0,1]$ , with  $C = 1$  implying a purely compressible flow.  
284 The importance of the presented definition of the measure of compressibility  $C$  is that it  
285 accounts for the finite-time correlations and its values are directly related to the ability of  
286 gathering the tracer particle into patches.

287 The scheme of calculations resembles a similar scheme used for the identification of  
288 semi-persistent patterns (Soomere et al. 2010). A longer time interval  $t_D$  of interest (year  
289 1991 in the calculations in this paper) is divided into time intervals (windows) with a length  
290 of  $t_w = 16$ – $96$  hours (Fig. 2). As mentioned above, one tracer is placed at the centre of each  
291 wet grid point of the RCO model and its displacement is traced over this window; usually  
292 over a number of time steps. The results of calculations over a particular time window form  
293 one realization of the process of changes to the area of surface elements. For a new  
294 realization, the simulations of the same pattern of tracers and surface elements are restarted  
295 with a time lag  $t_s = 1$  day.

296 After performing simulations for such a pool of realizations, we average the value of  $C$   
297 pointwise over different time spans: on daily, monthly, seasonal and yearly base. The  
298 resulting spatial maps characterize the spatial variations in the field compressibility for  
299 different time intervals over the Gulf of Finland. As discussed above, large values of  
300 compressibility in these maps show a predictive estimate of the likelihood of tracers inserted  
301 into various grid cells to gather into patches, equivalently, areas where high concentrations of  
302 floaters, garbage, adverse impacts, etc., are likely.

303 The above-mentioned property (that the basin-wide average 2D flow divergence is  
304 zero for a sea area of constant size) offers a way to judge to a certain degree about the  
305 correctness of the calculations. Figure 3 presents the average divergence, integrated over the  
306 entire area of the Gulf of Finland, as calculated for every day of year 1991 using the described  
307 technique with  $t_w = 4$  hours. The plot shows values which tend to be really close to zero  
308 throughout the year. The small variations reflect the surface water exchange between the area  
309 over which the divergence is calculated and the Baltic Proper. The mostly positive values  
310 apparently mirror the excess of fresh water inflow in this area (Leppäranta and Myrberg,



311 2009) while a few negative values evidently are connected with surface water inflow owing to  
312 specific wind events .

313

## 314 **5. Spatial distributions of compressibility**

315 The resulting maps vividly demonstrate that there exist areas with high compressibility  
316 values in the Gulf of Finland (Fig. 3). Most of these areas have an elongated stripe-like shape  
317 and are generally located close to the shore. Most likely the areas with a high compressibility  
318 reflect regions hosting intense vertical motions (upwelling or downwelling) in coastal areas,  
319 possibly with upwelling filaments, or divergence or convergence zones between coastal  
320 currents and offshore mesoscale circulation. For example, during the first week of November  
321 1991, the highest compressibility is found in the vicinity of the River Kymi mouth in SE part  
322 of the Gulf of Finland. This region, with local values of  $C$  up to 0.9, is also characterized by  
323 merging of the voluminous runoff of River Neva with waters coming from River Kymi and  
324 brackish waters of the Gulf of Finland and, thus, high values of  $C$  are not unexpected.

325 In contrast with the classical definition, our definition of compressibility makes it  
326 possible to calculate its dependence on the length of the time window used for estimates of  
327 the change to the area of surface elements. The use of very short time windows is equivalent  
328 to the calculation of pointwise compressibility. The use of longer time windows makes it  
329 possible to track the distortions of the surface elements over a certain sea area during their  
330 Lagrangian drift. This option allows identifying areas over which the compressibility  
331 increases cumulatively over some time interval. Such areas are actually the best candidates for  
332 emerging high concentrations of adverse impacts.

333 Calculations using different lengths of  $t_w$  show that, for shorter time windows (0 to 24  
334 hours), the resulting values of  $C$  are relatively low and generally do not reach the critical  
335 value of 0.5 (Fig. 5). With an increase in the time window to 48–72 hours, this threshold is  
336 reached at several locations (Figs. 6, 7).

337 The presented results demonstrate that the locations of the high-value regions of  $C$  are  
338 qualitatively the same for all choices of the time window length. The elongated areas of high  
339 compressibility may be interpreted as regions in which the compressibility cumulatively  
340 increases in the direction of the surface current. The critical values in  $C$  are usually reached  
341 only if the time window is 12 hours or longer. Remarkably, several elongated areas of high  $C$   
342 are oriented almost across the gulf. Such areas may reflect relatively intense cross-gulf  
343 transport pathways (Soomere et al. 2010) which also demonstrate systematic contraction or  
344 expansion. The quantitative results of the variation in the length of the time window are  
345 highlighted in Fig. 7 that shows the areas of the sea surface characterized by high (>0.5)  
346 values of  $C$ , obtained setting the time window to 48 hours, that wouldn't have been evident if  
347 the simulation was run on the same time interval using a shorter time window.

348 The areas characterized by high values of  $C$  seem to be affected by a strong seasonal  
349 variability (Fig. 9). For the year 1991, the maximum values of the finite-time compressibility  
350 (Table 1) are the largest in autumn (October–December) whereas the average values of  $C$   
351 exceed the patch-generation threshold of  $C=0.5$  at several locations. It is remarkable that the  
352 highest values of  $C$  near the mouth of the River Neva and at the entrance to the Gulf of  
353 Finland occur almost at the same locations as in simulations for one week (Fig. 3). This  
354 feature suggests that the areas favorable for the generation of patches may persist over several  
355 months.

356 Other seasons have clearly less maximum values of  $C$  that are close to the threshold of  
357  $C=0.5$  and even remain below this threshold for the spring months (April–June). The  
358 qualitative appearance of the field of  $C$  is very much the same in different seasons (Fig. 9).  
359 The life-time of high-value areas of compressibility seems to be limited to a few months:  
360 averaging over the entire year of 1991 leads to a substantial decrease in the local values of  $C$   
361 which remained well below the threshold in question.

## 362 6. Conclusions

363 The property of compressibility of a 2D velocity field overlying 3D circulation is a  
364 natural generalization of the impact of various phenomena (such as upwellings,  
365 downwellings, convergence or divergence of ocean currents, Langmuir circulation, etc.) that  
366 may lead on the formation of inhomogeneities in otherwise smooth fields in the surface layer.  
367 In other words, such processes may cause contraction or extension of the sea surface, in this  
368 way affecting the behavior of different substances floating on the sea surface. Their obvious  
369 consequence is the formation of patches.

370 The traditional definition of compressibility basically relies on instantaneous velocity  
371 fields and does not account for the time history of motions and cumulative distortion of sea  
372 surface. The modified measure of finite-time compressibility, introduced in this paper through  
373 tracking the local changes to the area of surface elements, makes it possible to systematically  
374 quantify the impact of the listed processes, independently on their particular physical origin,  
375 on various fields on the sea surface. It allows for variable-length time window averaging for  
376 flows translating surface elements over the sea surface. This property makes it possible to  
377 calculate cumulative effects of compressibility and, thus, to highlights sea regions  
378 characterized by large values of compressibility occurring during some finite time interval  
379 and which wouldn't have become evident using the classical definition. Another key feature of  
380 this measure is its tight relation with the ability of clustering of passive tracers in some  
381 regions of the sea surface, allowing hindcast and forecast of the domains in which the patch  
382 formation is most likely.

383 The particular values of this measure of compressibility to some extent depend on the  
384 length of time slices over which it is calculated. The spatial variations of the compressibility  
385 are fairly strong. While its values for short time slices are fairly low, for slices of quite  
386 reasonable length (48–72 hours) its values reach and overshoot the threshold for the formation  
387 of extensive patches. Usually coastal regions are characterized by significant compressibility  
388 values (above the critical level of 0.5) but comparable values area also found in elongated  
389 offshore areas. The spatial distributions of compressibility reveal extensive seasonal-scale  
390 variations. The performed simulations for one year (1991) suggest that several regions of high  
391 compressibility (equivalently, areas prone to the generation of surface patches) persist, at  
392 least, during a few months but apparently are smoothed out when averaged over entire year.  
393 Finally, we mention that this study only focuses on mesoscale variations in the  
394 compressibility and does not cover compressibility of small-scale structures (<2 nautical  
395 miles), which can greatly enhance the effect of patchiness (Granskog et al., 2005) and will be  
396 the subject of further studies.

397

398 **Acknowledgements.** This study was supported by the Estonian Science Foundation (grants  
399 No. 7413 and 7909), targeted financing by the Estonian Ministry of Education and Research  
400 (grant SF0140007s11) and the BalticWay project, which was supported by funding from the  
401 European Community's Seventh Framework Programme (FP/2007–2013) under grant  
402 agreement No. 217246 made with the joint Baltic Sea research and development programme

403 BONUS. AG is supported by the support programme for international doctoral studies in  
404 Estonia DoRa.

405 **References**

406 Alenius, P., Nekrasov, A., Myrberg K., 1998. Physical oceanography of the Gulf of Finland: a  
407 review. *Boreal Environ. Res.* 3(2), 97–125.

408 Anderson, D., Balmaseda, M., Vidard, A., 2006. The ECMWF perspective, in: Chassignet,  
409 E.P., Verron, J. (Eds.), *Ocean weather forecasting: an integrated view of oceanography*.  
410 Springer, Dordrecht, pp. 361–379.

411 Andrady, A. L., 2011. Microplastics in the marine environment. *Marine Pollut. Bull.* 62 (8),  
412 1596–1605.

413 Bec, J., Gawedzki, K., Horvai, P., 2004. Multifractal clustering in compressible flows. *Phys.*  
414 *Rev. Lett.* 92(22), Art. No. 224501.

415 Blanke, B., Raynard, R., 1997. Kinematics of the Pacific Equatorial Undercurrent: an  
416 Eulerian and Lagrangian approach from GCM results. *J. Phys. Oceanogr.* 27 (6), 1038–1053.

417 Boffetta, G., Davoudi, J., Eckhardt, B., Schumacher, J., 2004. Lagrangian tracers on a surface  
418 flow: The role of time correlations. *Phys. Rev. Lett.* 93 (13), Art. No. 134501.

419 Burchard, H., Floeser, G., Staneva, J.V., Badewien, T.H., Riethmueller, R., 2008. Impact of  
420 density gradients on net sediment transport into the Wadden Sea. *J. Phys. Oceanogr.* 38 (3),  
421 566–587.

422 Burchard, H., Bolding, K., Villarreal, M.R., 2004. Three-dimensional modelling of estuarine  
423 turbidity maxima in a tidal estuary. *Ocean Dyn.* 54 (2), 250–265.

424 Cressman, J.R., Davoudi, J., Goldberg, W.I., Schumacher, J., 2004. Eulerian and Lagrangian  
425 studies in surface flow turbulence. *New J. Phys.* 6, Art. No. 53.,

426 De Vries, P., Döös, K., 2001. Calculating Lagrangian trajectories using time-dependent  
427 velocity fields. *J. Atmos. Ocean. Techn.* 18 (6), 1092–1101.

428 Döös, K., 1995. Inter-ocean exchange of water masses. *J. Geophys. Res. Oceans*, 100 (C7),  
429 13499–13514.

430 Falkovich, G., Gawedzki, K., Vergassola, M., 2001. Particles and fields in fluid turbulence.  
431 *Rev. Mod. Phys.*, 73 (4), 913–975.

432 Fine, R. A., Millero, F. J., 1973. Compressibility of fluids as a function of temperature and  
433 pressure. *J. Chem. Phys.*, 59 (10), 5529–5536.

434 Garrison, T.S., 2011. *Essentials of oceanography*, 5th ed. Brooks Cole, Pacific Grove.

435 Gerdes, R., Köberle, C., Willebrand, J., 1991. The influence of numerical advection schemes  
436 on the results of ocean general circulation models. *Clim. Dyn.* 5, 211–226.

437 Granskog, M., Kaartokallio, H., Kuosa, H., Thomas, D., Ehn, J., Sonninen, E., 2005. Scales of  
438 horizontal patchiness in chlorophyll a, chemical and physical properties of landfast sea ice in  
439 the Gulf of Finland (Baltic Sea). *Polar Biology* 28 (4), 276–283.

440 Held, I.M., Pierrehumbert, R.T., Garner, S.T., Swanson, K.L. 1995. Surface quasi-geostrophic  
441 dynamics. *J. Fluid Mech.*, 282, 1–20.

442 Hibler, W., 1979. A dynamic thermodynamic sea ice model. U.S. Army Cold Regions  
443 Research and Engineering Laboratory , p. 815-846.

- 444 Hunke, E.C., Dukowicz J.K., 1997. An elastic-viscous-plastic model for sea ice dynamics. *J.*  
445 *Phys. Oceanogr*, 27, 1849–1868.
- 446 Kalda, J. 2000. Simple model of intermittent passive scalar turbulence. *Phys. Rev. Lett.* 84  
447 (3), 471–474.
- 448 Kalda, J. 2007. Sticky particles in compressible flows: aggregation and Richardson's Law.  
449 *Phys. Rev. Lett.* 98 (6), Art No. 064501.
- 450 Killworth, P., Stainforth, D., Webb, D., Paterson, S., 1991. The development of a free-surface  
451 Bryan-Cox-Semtner ocean model. *J. Phys. Oceanogr.*, 21. 1333–1348.
- 452 Kononen, K., Nömmann, S., Hansen, G., Hansen, R., Breuel, G., Gupalo, E.N., 1992. Spatial  
453 heterogeneity and dynamics of vernal phytoplankton species in the Baltic Sea in April-May  
454 1986. *J. Plankton Res.*, 14 (1) 107–125.
- 455 Kraichnan, R.H., Montgomery, D., 1980. Two-dimensional turbulence. *Repts. Progr. Phys.* 43  
456 (5), 548–619.
- 457 Lee, D.K., Niiler, N., 2010. Influence of warm SST anomalies formed in the eastern Pacific  
458 subduction zone on recent El Niño events. *J. Marine Res.*, 68 (3-4), 459–477.
- 459 Lehmann, A., Myrberg, K., 2008. Upwelling in the Baltic Sea – A review. *J. Marine Sys.* 74,  
460 S3–S12.
- 461 Leppäranta, M., Myrberg, K., 2009. *The physical oceanography of the Baltic Sea.* Springer,  
462 Berlin Heidelberg.
- 463 Meier, H.E.M., 2001. On the parametrization of mixing in three-dimensional Baltic Sea  
464 models. *J. Geophys. Res.* 106 (C12), 30,997–31,016.
- 465 Meier H.E.M., Doscher, R., Faxen, T, 2003. A multiprocessor coupled ice-ocean model for  
466 the Baltic Sea: application to salt inflow. *J. Geophys. Res.* C106, C30,997–C31,016.
- 467 Meier, H.E.M., 2007. Modeling the pathways and ages of inflowing salt- and freshwater in  
468 the Baltic Sea. *Estuar. Coast. Shelf Sci.* 74 (4), 610–627.
- 469 Ollitrault, M., Gabillet, C. and Colin de Verdière, A. 2005. Open ocean regimes of relative  
470 dispersion. *J. Fluid Mech.* **533**, 381–407.
- 471 Perlekar, P., Benzi, R., Nelson, D., Toschi F. 2010. Population dynamics at high Reynolds  
472 number. *Phys. Rev. Lett.* 105 (14), Art. No. 144501.
- 473 Powell, T.M., Okubo, A. 1994. Turbulence, diffusion and patchiness in the sea. *Phil. Trans.*  
474 *Roy. Soc. London B*, 343 (1303), 11–18.
- 475 Pichel, W.G., Churnside, J.H., Veenstra, T.S., Foley, D.G., Friedman, K.S., Brainard, R.E.,  
476 Nicoll, J.B., Zheng, Q., Clemente-Colon, P., (2007). Marine debris collects within the North  
477 Pacific Subtropical convergence zone. *Mar. Poll. Bull.* 54 (8), 1207–1211.
- 478 Rhines, P., 1979. Geostrophic turbulence. *Ann. Rev. Fluid Mech.* 11, 401–441.
- 479 Richards, Z.T., Beger M., 2011. A quantification of the standing stock of macro-debris in  
480 Majuro lagoon and its effect on hard coral communities. *Mar. Poll. Bull.* 62 (8), 1693–1701.
- 481 Richardson, L.F., 1926- Atmospheric diffusion shown on a distance-neighbor graph. *Proc.*  
482 *Roy. Soc. A* **110**, 709–737.
- 483 Samuelsson, P., Jones, C.G., Willén, U., Ullerstig, A., Gollvik, S., Hansson, U., Jansson, C.,  
484 Kjellström, E., Nikulin, G., Wyser, K., 2011, The Rossby Centre Regional Climate Model  
485 RCA3: Model description and performance. *Tellus A* 63, 4–23.

- 486 Schilling, K., Zessner, M., 2011. Foam in the aquatic environment. *Water Res.* 45 (15), 4355–  
487 4366.
- 488 Schumacher, J., Eckhardt, B. 2002. Clustering dynamics of Lagrangian tracers in free-surface  
489 flows. *Phys. Rev. E*, 66 (1), Art. No 017303.
- 490 Soomere, T., Viikmäe, B., Delpeche, N., Myrberg, K., 2010. Towards identification of areas  
491 of reduced risk in the Gulf of Finland. *Proc. Estonian Acad. Sci.* 59 (2) 156–165.
- 492 Soomere, T., Andrejev, O., Sokolov, A., Myrberg, K., 2011. The use of Lagrangian  
493 trajectories for identification the environmentally safe fairway. *Mar. Poll. Bull.* 62 (7), 1410–  
494 1420.
- 495 Stevens, D.P., 1991. The open boundary condition in the United Kingdom Fine-Resolution-  
496 Antarctic-Model. *J. Phys. Oceanogr.*, 21 (9), 1494–1499.
- 497 Thorpe, S.A., 2009. Spreading of floating particles by Langmuir circulation, *Mar. Poll. Bull.*  
498 58 (12), 1787–1791.
- 499 Vucelja, M., Falkovich, G., Fouxon, I. 2007. Clustering of matter in waves and currents.  
500 *Phys. Rev. E* 75 (6), Art. No. 065301.
- 501 Webb, D.J, Coward, A.C., de Cuevas B.A., Gwilliam G.S. 1997. A Multiprocessor Ocean  
502 General Circulation Model Using Message Passing. *J. Atmos. Oceanic Technol.* 14, 175-183.

503

#### 504 **Figure captions**

505

506 Figure 1. Scheme of the selection of surface elements and their distortions in time

507 Figure 2. Definition sketch of splitting the simulation period into time windows.

508 Figure 3. Divergence of the 2D flow on the sea surface, integrated over the entire Gulf of  
509 Finland, the Baltic Sea, throughout year 1991.

510 Figure 4. Average compressibility of water surface in the Gulf of Finland for one week in  
511 November 1991 calculated using  $t_w=48$  hours.

512 Figure 5. Average compressibility of water surface in the Gulf of Finland for one week in  
513 April 1991, calculated with the time window of 24 hours.

514 Figure 6. Average compressibility of water surface in the Gulf of Finland for one week in  
515 April 1991, calculated with the time window of 48 hours.

516 Figure 7. Average compressibility of water surface in the Gulf of Finland for one week in  
517 April 1991, calculated with the time window of 72 hours.

518 Figure 8. Areas (green) in which the finite-time compressibility exceeds 0.5 in a simulation  
519 with  $t_w=72$  hours compared to a simulation with  $t_w=48$  hours during the first week of  
520 November 1991.

521 Figure 9. Average compressibility of water surface in the Gulf of Finland in winter and  
522 autumn 1991.

523

#### 524 **Table captions**

525 Table 1. Maximum values of finite-time compressibility  $C$  calculated using  $t_w$  for different  
526 seasons in the Gulf of Finland.

# On the compressibility of the surface currents in the Gulf of Finland, the Baltic Sea

Jaan Kalda, Tarmo Soomere, Andrea Giudici

## Figures

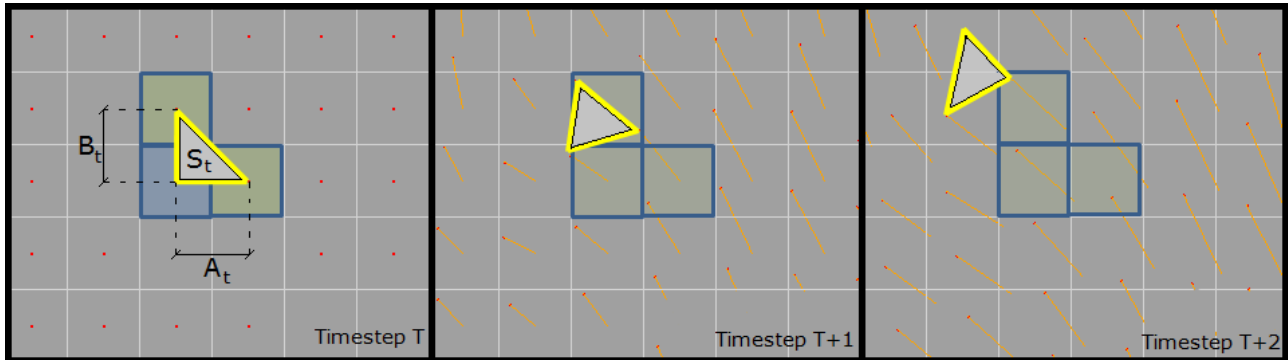


Figure 1. Scheme of the selection of surface elements and their distortions in time

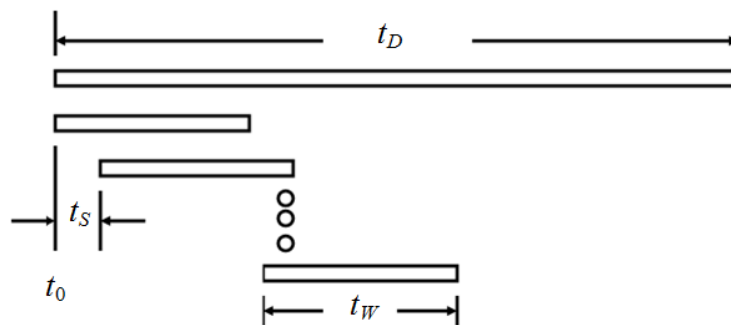


Figure 2. Definition sketch of splitting the simulation period into time windows.

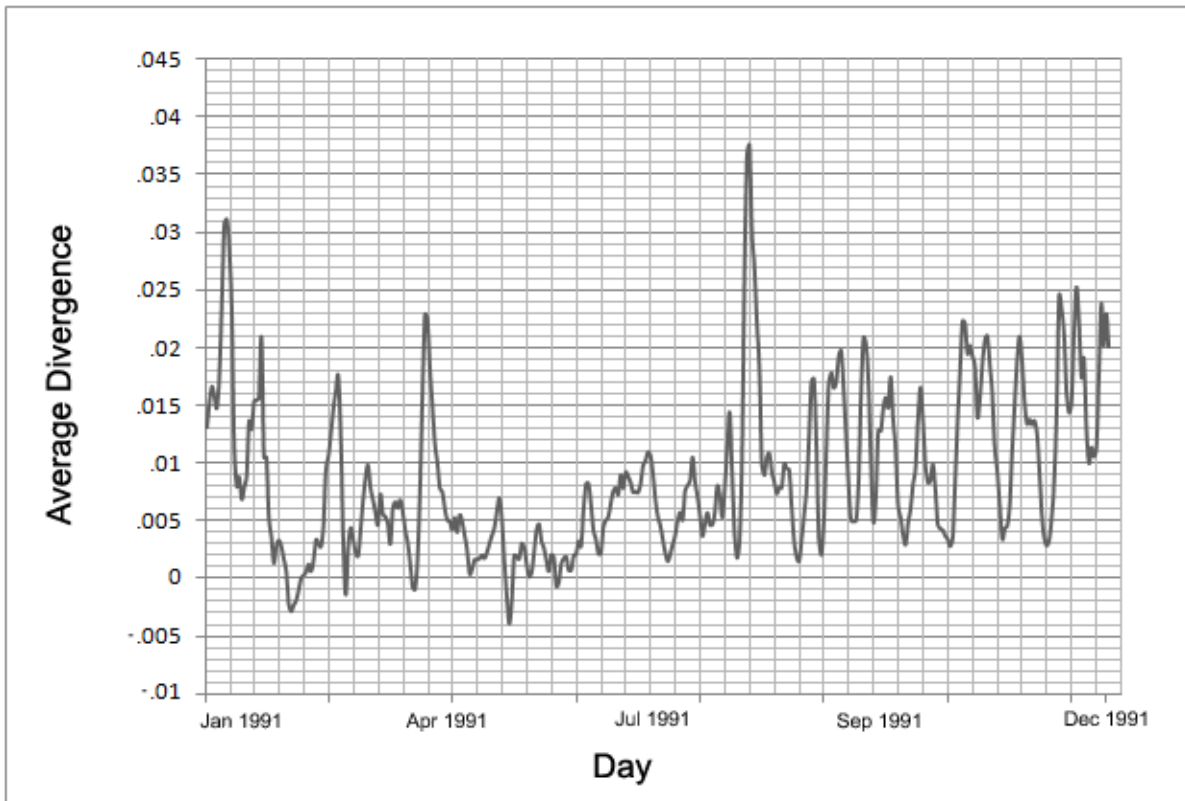


Figure 3. Divergence of the 2D flow on the sea surface, integrated over the entire Gulf of Finland, the Baltic Sea, throughout year 1991.



Figure 4. Average compressibility of water surface in the Gulf of Finland for one week in November 1991 calculated using  $t_w = 48$  hours.



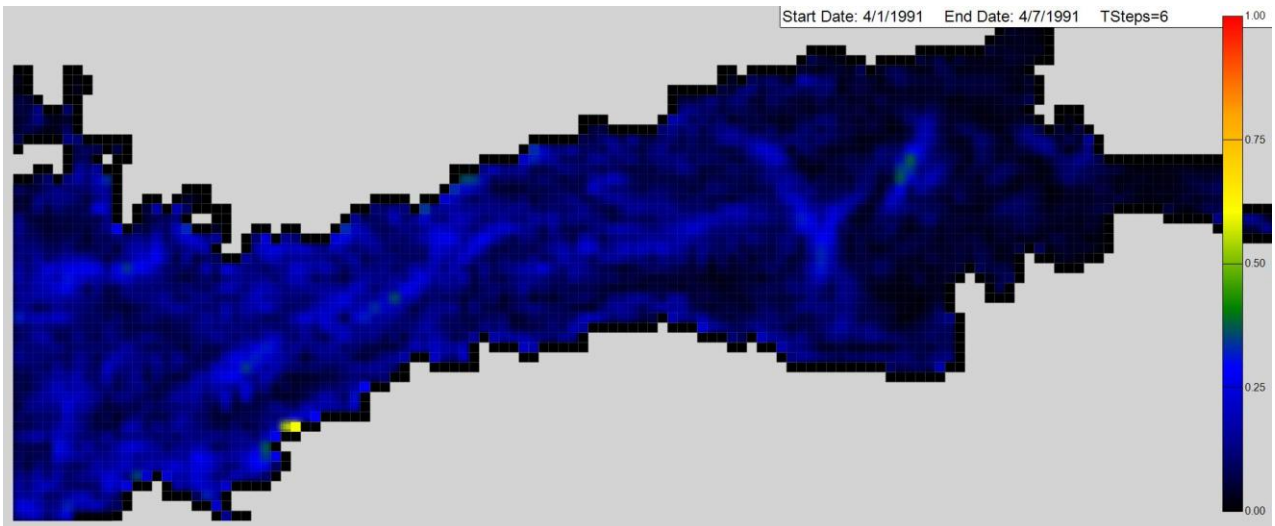


Figure 5. Average compressibility of water surface in the Gulf of Finland for one week in April 1991, calculated with the time window of 24 hours.

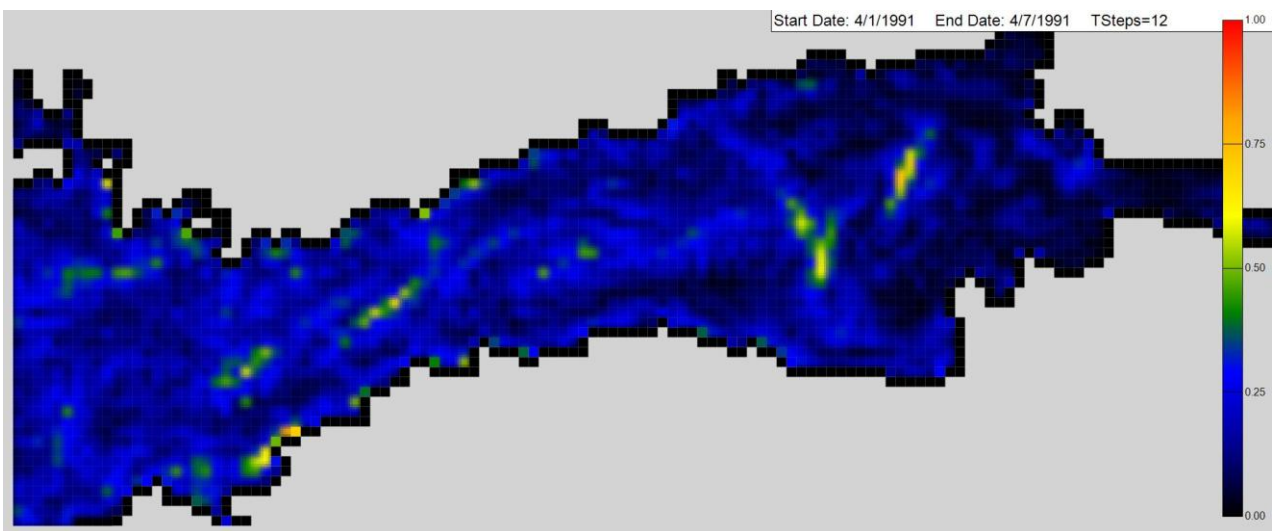


Figure 6. Average compressibility of water surface in the Gulf of Finland for one week in April 1991, calculated with the time window of 48 hours.

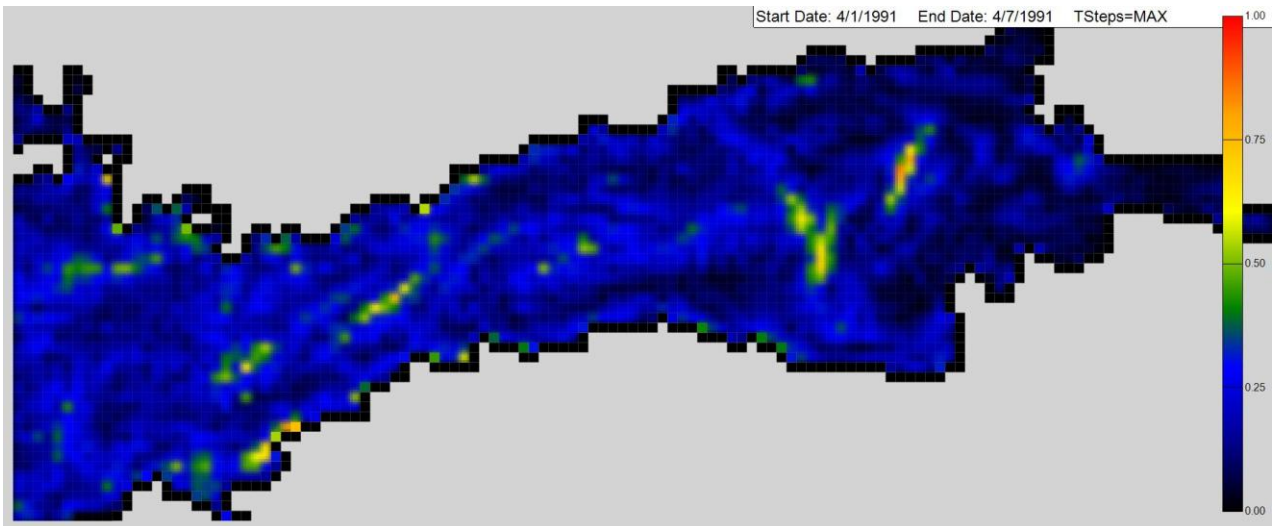


Figure 7. Average compressibility of water surface in the Gulf of Finland for one week in April 1991, calculated with the time window of 72 hours.

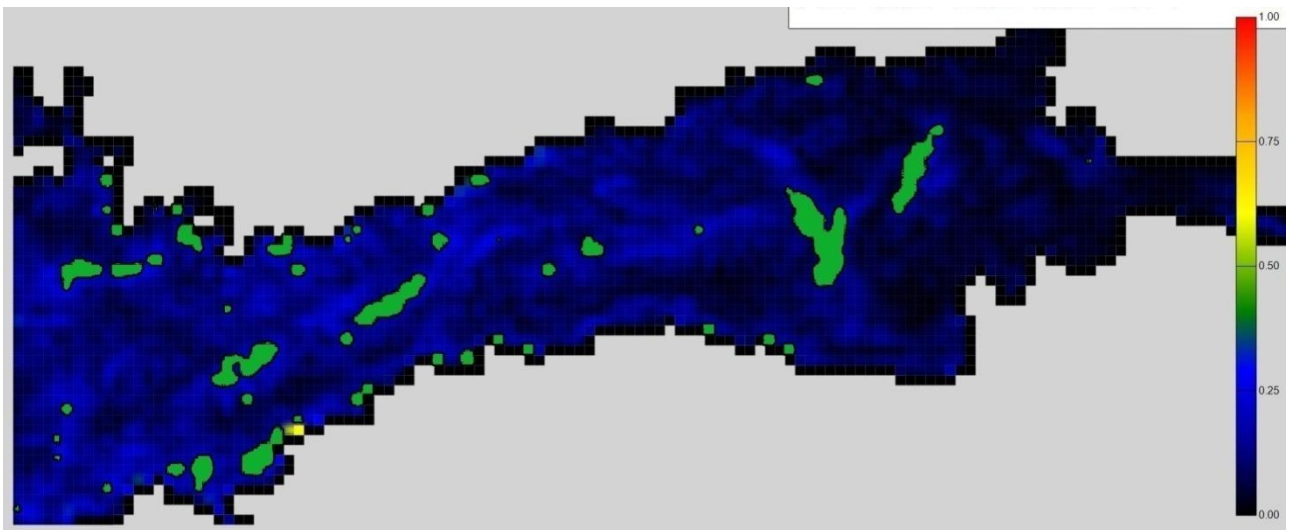


Figure 8. Areas (green) in which the finite-time compressibility exceeds 0.5 in a simulation with  $t_w = 72$  hours compared to a simulation with  $t_w = 48$  hours during the first week of November 1991.

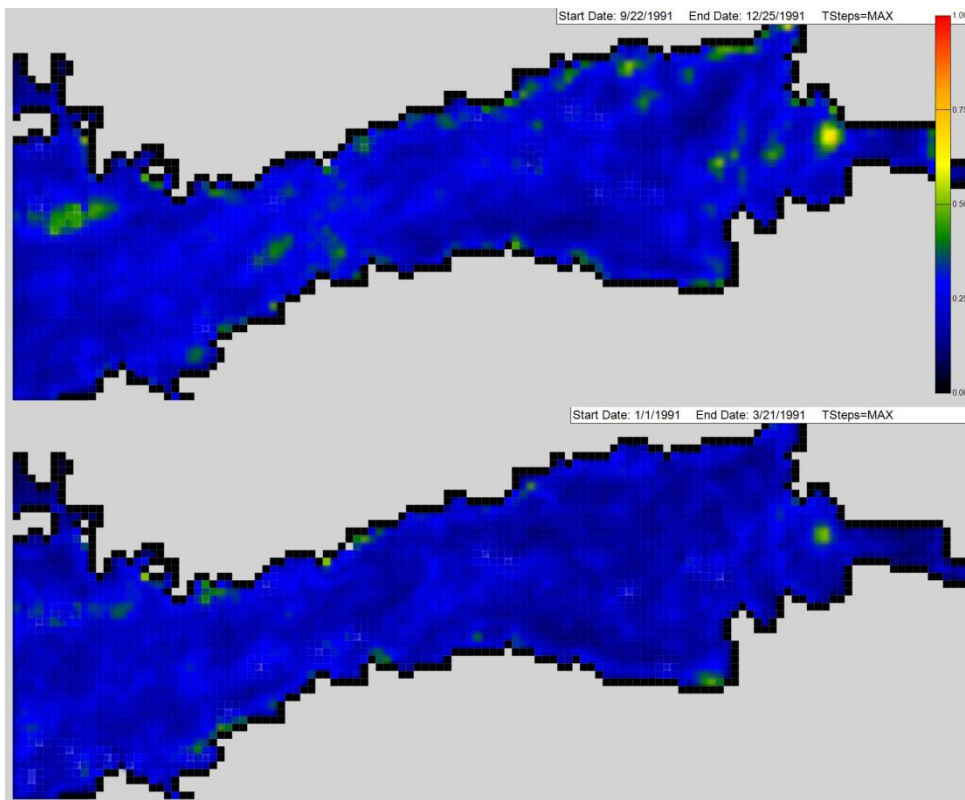


Figure 9. Average compressibility of water surface in the Gulf of Finland in winter and autumn 1991.

# On the compressibility of the surface currents in the Gulf of Finland, the Baltic Sea

Jaan Kalda, Tarmo Soomere, Andrea Giudici

Table 1. Maximum values of finite-time compressibility  $C$  calculated using  $t_w$  for different seasons in the Gulf of Finland.

Season	Maximum compressibility
Spring 1991	0.4408
Summer 1991	0.5246
Autumn 1991	0.7634
Winter 1991	0.5072